The higher relative concentration of K⁺ to Na⁺ in saline water improves soil hydraulic conductivity, salt leaching efficiency and structural stability

Sihui Yan [a, b], Tibin Zhang [a, c, *], Binbin Zhang [a, b], Tonggang Zhang [a, b], Yu Cheng [a, b],

Chun Wang [a, b], Min Luo [a, b], Hao Feng [a, c], Kadambot H.M. Siddique [d]

[a.] Key Laboratory of Agricultural Soil and Water Engineering in Arid and Semiarid Areas, Ministry of Education, Northwest A&F University, Yangling, Shaanxi 712100, P. R. China

[b.] College of Water Resources and Architecture Engineering, Northwest A&F University, Yangling, Shaanxi 712100, P. R. China

[c.] Institute of Soil and Water Conservation, Northwest A&F University, Yangling, Shaanxi 712100, P. R. China

[d] The UWA Institute of Agriculture, The University of Western Australia, Perth, WA 6001, Australia

* Corresponding author at: Institute of Soil and Water Conservation, Northwest A&F University, Yangling, Shaanxi 712100, China. Tel.: +86 29 87012871; fax: +86 29 87011354. E-mail: zhangtibin@163.com (T. Zhang)

18   **Abstract**

19   Soil salinity and sodicity caused by saline water irrigation are widely observed

20   globally. Clay dispersion and swelling are influenced by sodium (Na^+) concentration

21   and electrical conductivity (EC) of soil solution. Specifically, soil potassium (K^+) also

22   significantly affects soil structural stability, but which concern was rarely addressed in

23   previous studies or irrigation practices. A soil column experiment was carried out to

24   examine the effects of saline water with different relative concentrations of K^+ to Na^+

25   (K^+/Na^+), including K^+/Na^+ of 0:1 (K0Na1), 1:1 (K1Na1), 1:0 (K1Na0) at a constant

26   EC (4 dS m^{-1}), and deionized water as the control (CK), on soil physicochemical

27   properties. The results indicated that at the constant EC of 4 dS m^{-1}, the infiltration rate

28   and water content were significantly (P < 0.05) affected by K^+/Na^+ values, K0Na1,

29   K1Na1 and K1Na0 significantly (P < 0.05) reduced saturated hydraulic conductivity by

30   43.62%, 29.04% and 18.06% respectively compared with CK. The volumetric water

31   content was significantly (P < 0.05) higher in K0Na1 than CK at both 15 and 30 cm soil

32   depths. K1Na1 and K1Na0 significantly (P < 0.05) reduced the desalination time and

33   required leaching volume. K0Na1 and K1Na1 reached the desalination standard after

34   the fifth and second infiltration, respectively, as K1Na0 did not exceed the bulk

35   electrical conductivity required for desalination prerequisite throughout the whole

36   infiltration cycle at 15 cm soil layer. Furthermore, due to the transformation of

37   macropores into micropores spurred by clay dispersion, soil total porosity in K0Na1

38   dramatically decreased compared with CK, and K1Na0 even increased the proportion

39   of soil macropores. The higher relative concentration of K^+ to Na^+ in saline water was

40   more conducive to soil aggregates stability, alleviating the risk of macropores reduction

41   caused by sodicity.

42   **Keywords:** Saline water; Cation composition; Hydraulic properties; Desalination; Pore

43   structure.

44   **1 Introduction**

45   Freshwater shortage resulted from elevated demand for water resources as well as

46   the irrational exploitation and use after economic and population growth (Zhang and

47   Xie 2019; Prajapati et al. 2021), constrains the sustainability of agricultural production

48   (Aparicio et al., 2019). Alternative water resources with variable water quality (such as

49   saline water) are being considered for agricultural irrigation in several desert and saline

50   areas (Singh et al. 2021; Liu et al. 2022a). Utilizing saline water could partly alleviate

51   the undersupply of freshwater for agricultural production (Yang et al., 2020). However,

52   the other side of the coin is that saline water irrigation could result in soil salinization

53   and/or sodicity. Once the soil is salinized and/or alkalized, soil hydraulic properties,

54   like infiltration rate, saturated hydraulic conductivity and permeability, will change

55   inevitably (Scudiero et al., 2017). And cations in the soil solution change the soil

56   structural characteristics through the soil clay particle dispersion and flocculation

57   (Bouksila et al. 2013; Hack-ten Broeke et al. 2016; Zhang et al. 2018). Therefore, in

58   order to optimize saline water utilization, the effects of saline water quality on the soil

59 hydraulic properties and pore structure characteristics should be paid more attention.

60   Saline water irrigation can increase the monovalent ions concentration in soil

61 solution and affect soil structure (Qadir et al. 2007; Qadir et al. 2021). Excess sodium

62 (Na^+) from saline irrigation water is adsorbed onto the clay surface in salt-affected soils

63 where sodium compounds predominate contributing to the disintegration of soil

64 structure (Marchuk and Rengasamy 2011; Belkheiri and Mulas 2013; Awedat et al.

65 2021). As percolation progresses, the thickness of the diffusion double electron layers

66 increases due to the relatively larger hydrated radius of Na^+, and the repulsive force

67 between adjacent diffusion double electron layers appears to increase, resulting in the

68 dispersion and swelling of soil particles (Alva et al. 1991; Reading et al. 2015).

69   Soil calcium (Ca^{2+}) and magnesium (Mg^{2+}) can alleviate soil dispersibility by

70 replacing Na^+ in soil colloids, the outer layers of the Ca^{2+} and Mg^{2+} containing colloidal

71 particles do not adsorb water molecules, turning Na^+ qualitative hydrophilic colloid into

72 Ca^{2+} and Mg^{2+} hydrophobic colloids (Marchuk and Rengasamy 2011; Tsai et al. 2012).

73 Colloidal particles move closer to each other, promoting soil particles forming water

74 stable aggregates, thus improving soil structural stability (Gharaibeh et al. 2009;

75 McKenna et al. 2019). Therefore, the concentration of Na^+ in relation to Mg^{2+} and Ca^{2+}

76 (sodium adsorption ratio, SAR) (U.S. Salinity Laboratory Staff 1954) is a crucial

77 criterion for soil structural stability and hydraulic conductivity (Rengasamy and

78 Marchuk 2011). Although SAR can be used to predict soil clay dispersion effect caused

79 by cations, the controlling mechanism of dispersion in SAR is presumed to be

80   exchangeable Na^+. However, Na^+ does not alone cause soil dispersion since the

81   chemical component of clay structure integrity is mainly a function of ionic valence

82   and hydration radius (Marchuk et al., 2014). Potassium (K^+) has been overlooked

83   because salt-affected soils typically contain low amounts of K^+. However, Li et al.

84   (2022) reported that under the continuous recycling use of underground saline water,

85   water-soluble and exchangeable K^+ is higher than Ca^{2+} and Mg^{2+} in the Hetao irrigation

86   district—one of the large irrigation districts in China. It is anticipated that the long-term

87   use of irrigation water with high K^+ concentrations may therefore create substantial

88   challenges in preserving good soil structure and adequate infiltration rates (Sposito et

89   al., 2016). K^+ is not as effective as Na^+ in generating soil particle dispersion and

90   swelling problems, yet Marchuk and Marchuk (2018) pointed out that K^+ could

91   substitute Na^+ on exchange sites to encourage Na^+ leaching and increase water

92   conductivity to some extent. A lower concentration of K^+ may have positive effects on

93   soil permeability due to the substitution of exchangeable Na^+ by K^+ with lower

94   dispersive potential, increasing aggregates stability and soil pore connectivity (Buelow

95   et al., 2015). Traditional SAR ignored the role of K^+, a newly proposed equation, cation

96   ratio of soil structural stability (CROSS) could integrate the effects of Na^+ and K^+ in

97   soil, which is an important indicator for assessing the quality of saline water

98   (Rengasamy and Marchuk 2011).

99   Thus, we hypothesized that the amount of K^+ relative to Na^+ would certainly have

100   an effect on soil structural stability, which could be evaluated in a column experiment

101   under controlled conditions. The specific objectives of this study were to (1) ascertain

102   the effect of irrigation saline water with different relative concentrations of K^+ to Na^+

103   (K^+/Na^+) on transport and distribution of water and salt; (2) determine the effect on soil

104   pore structural characteristics; (3) predict these effects using a newly proposed index

105   (CROSS) rather than SAR.

106   **2 Materials and methods**

107   **2.1 Soil sampling location and properties**

108   The study soil was collected from a layer of 0–40 cm field in Yangling (108°04′E,

109   34°20′N), Shaanxi Province, China. After air-dried, the soil was grounded to pass

110   through a 2-mm seize. Soil's physical and chemical properties are listed in Table 1. Soil

111   particle size distribution was measured by the Laser Mastersizer 2000 (Malvern

112   Instruments, Malvern, UK), and according to the international classification system,

113   soil texture was classified as silty clay. Soil bulk density was calculated usnig the soil

114   core method. EC_e and pH were measured using conductivity meter (DDS-307, China)

115   and pH meter (PHS-3C, China), respectively. Total soluble salts refer to the total

116   amount of soluble salts in soil-saturated paste extract. Flame photometry (6400A, China)

117   was used to measure soluble Na^+ and K^+, concentrations of CO_3^{2-} and HCO_3^- were

118   tested using the neutral titration method, Cl^- was analyzed using the silver nitrate

119   titration method, and SO_4^{2-} was determined using barium sulfate turbidimetric method,

120   Mg^{2+} and Ca^{2+} were specified using ethylene diamine tetraacetic acid (EDTA)

121   titrimetric method (Bao 2005).

122   Table 1 The physicochemical properties of study soil.

Property	Value
Particle size distribution (%)	
Sand (> 0.05 mm)	8.10
Silt (0.05–0.002 mm)	60.62
Clay (< 0.002 mm)	31.28
Texture	Silty clay
EC_e (dS m^{-1})	0.72
pH	7.66
Total soluble salts (g Kg^{-1})	0.14
Ion concentration (mmol L^{-1})	
$CO_3^{2-}+HCO_3^-$	0.60
Cl^-	0.23
SO_4^{2-}	2.18
Mg^{2+}	0.32
Ca^{2+}	0.54
Na^+	0.10
K^+	< 0.01

123   Note: EC_e is electrical conductivity of soil-saturated extract.

124   **2.2 Experimental design**

125   Soil columns were prepared using transparent polyvinyl chloride cylinders, with

126   an internal diameter of 20 cm and a height of 50 cm (Fig. 1). Round and small holes (6

127   mm diameter) were arranged equally at the bottom of each cylinder for drainage. A 5

128   cm depth quartz sand was laid at the bottom of the soil column as a filter layer before

129   packing to prevent small soil particles from being washed away. After that, air-dried

130   soil was packed at 40 cm height with a bulk density of 1.35 g cm^{-3} (referring to the

131   original level of the soil). The sieved dry soil was poured into each soil column in the

132   5-cm sections for uniform compaction, and the layer's surface was roughened to ensure

133   a tight connection to the next layer. The soil column was then allowed to stand in the

134   laboratory for 24 hours before starting the experiments described herein. The constant

135   water head (2 cm, using a Mariotte bottle) infiltration experiment was conducted with

136   3 replications for each treatment.
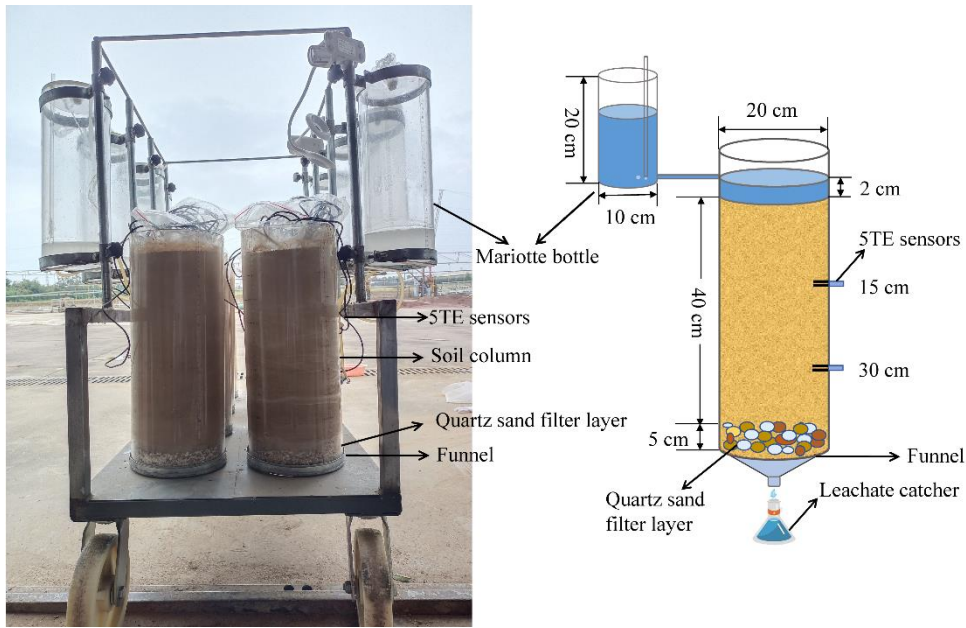
137

138   Fig. 1. Illustration of the experiment apparatus (a) and schematic diagram (b).

139   Three infiltration solutions were prepared with different ratios of K^+/Na^+ [(0:1

140   (K0Na1), 1:1 (K1Na1), 1:0 (K1Na0)] at constant EC of 4 dS m^{-1}, with deionized water

141   was used as the control (CK) (Table 2). The cation ratio of soil structural stability

142   (CROSS) (Rengasamy and Marchuk 2011) is an indicator of soil structural behavior as

143   influenced by both Na^+ and K^+, and it was calculated as follows (Smith et al., 2015):

144                      $$CROSS = \frac{Na^+ + 0.335K^+}{\left[\left(Ca^{2+} + 0.0758Mg^{2+}\right)/2\right]^{0.5}} \qquad (1)$$

145   where the chemical element symbols denote charge concentrations (mmol$_c$ L^{-1}).

146   Table 2 Saline water settings with different K^+/Na^+ at a constant EC.

Treatment	Added salt/ (mmol L^{-1})			K^+/Na^+	Setting EC (dS m^{-1})	Measured EC (dS m^{-1})	CROSS (mmol$_c$ L^{-1})$^{0.5}$
	KCl	NaCl	CaCl$_2$				
K0Na1	0	34	3	0:1	4.00	4.25	27.76
K1Na1	17	17	3	1:1	4.00	4.33	17.49
K1Na0	34	0	3	1:0	4.00	4.40	7.22
CK	Deionized water			/	0.00	0.02	/

147   Note: K0Na1, K1Na1 and K1Na0 indicate the saline water at EC of 4 dS m^{-1} with

148   K^+/Na^+ of 0:1, 1:1 and 1:0, respectively; CK, deionized water; CROSS represents cation

149   ratio of soil structural stability.

150   The experiment implemented alternate leaching, as the prolonged leaching process

151   of soil substrates is more helpful in illuminating the function of electrolyte effect and

152   cation exchange (Shaygan et al., 2017). The next infiltration was performed two days

153   after the drainage of the previous infiltration was completed. Soil layers were regarded

154   as reaching desalination prerequisite when the soil salt content came to less than 0.3%,

155   which meant that bulk electrical conductivity was less than 1.5 dS m^{-1} (transformation

156   from salt content to bulk electrical conductivity) (Yin et al., 2022). Water application

157   was stopped when the bulk electrical conductivity of all treatments at 15 cm depth

158   reached the prerequisite for desalination. This experiment was planned to fill all the

159   pores in the soil column throughout the infiltration cycle, therefore the water applied at

160   the first infiltration was described by the pore volume equation (Xu and Huang 2010):

161    $$V_p = V_s \cdot TP \tag{2}$$

162    $$TP = \frac{ds - BD}{ds} \tag{3}$$

163   where V_p is the pore volume (cm^3), V_s is the volume of filled soil (cm^3), TP is the soil

164 total porosity (%), ds is the soil particle density (2.65 g cm^{-3}) (Xu and Huang 2010),

165 BD is the bulk density (g cm^{-3}). According to Eq. (2) and Eq. (3), around 6 L of water

166 was required in the first infiltration. Required water volume for each subsequent

167 leaching was determined by the volume of leachate at the first infiltration, 0.5 L each

168 time.

169 **2.3 Soil properties measurements**

170 During the whole experimental period, soil volumetric water content and bulk

171 electrical conductivity were real-time monitored at 15 and 30 cm soil depths from the

172 soil surface by capacitance sensors (ECH2O 5TE, METER Group, USA) (Fig. 1).

173 Leachate was collected in the leachate catcher below the soil column. Cumulative

174 leachate volume was monitored over time to determine the saturated hydraulic

175 conductivity (K_{sat}, cm min^{-1}) of each treatment by using a derivation of Darcy's

176 approach (Sahin et al., 2011):

177
$$K_{sat} = \frac{V_l \cdot H}{A \cdot t \cdot (H + h)} \tag{4}$$

178 where V_l is the leachate volume (cm^3), H is the length of filled soil (cm), A is the surface

179 area of soil column (cm^2), t is the leaching time of measurement (min), h is the height

180 of constant water head (cm).

181 To determine the amount of salt released, we measured the volume and EC of the

182 leachate. The leachate was collected at 3 h intervals when the leachate started to drain,

183 and leachate was stored in 100 ml wide-mouth polypropylene reagent bottles. The salt

184   accumulated in the soil column was determined by subtracting the salt in the leachate

185   from the applied water, the salination rate (Rs, %) indicated the ratio of salt accumulated

186   in the soil column at every time of infiltration to the salt content at the first applied

187   water. Leaching efficiency (Le, g L^{-1}) refers to the amount of desalination per unit of

188   water volume in the desalination process. Rs and Le were calculated as follows:

189 $$Rs = m_s / m_w \qquad (5)$$

190 $$Le = (m_s - m_1) / w \qquad (6)$$

191   Where m_s is the salt content accumulated in soil column at each infiltration (g), m_w is

192   the salt content in the total water used for the first infiltration (g), m_1 is the mass of salts

193   after the first infiltration (g), w is the total water volume used for leaching (L).

194   Soil samples were collected from each soil column at 5-cm intervals with the 0–

195   40 cm soil layer three days after the final infiltration. Soil BD was calculated using the

196   soil core method, and TP was calculated by Eq. (3) based on BD. Soil water

197   characteristics curve was measured with the high velocity centrifugal method (CR21

198   Hitachi, Japan), and calibrated by RETC software (PC Progress Inc., Prague, Czech

199   Republic). Currently, several defining sizes of macropores are proposed, rather than a

200   precise definition and pore size range (Cameira et al. 2003; Kim et al. 2010; Hu et al.

201   2018; Budhathoki et al. 2022; Aldaz-Lusarreta et al. 2022). In this study, macropores

202   were defined as the pores with diameters larger than 1 mm, whereas micropores were

203   defined as smaller than 1 mm (Luxmoore 1981; Wilson and Luxmoore 1988). Based on

204   the capillary pressure data, the relationship between pore diameter (d, mm) and water

205   suction (S, Pa) was described according to the capillary bundle model (Jury et al., 1991):

206
$$d = \frac{300}{S} \tag{7}$$

207   **2.4 Statistical analysis**

208   Statistical analysis among all treatments with different K^+/Na^+ was performed in

209   SPSS 22.0 software, using one-way analysis of variance (ANOVA) based on the least

210   significant difference (LSD) test at 95% significance level (P < 0.05). All figures were

211   created through Origin 2022b.

212   **3 Results**

213   **3.1 Soil saturated hydraulic conductivity (K_{sat})**

214   The K0Na1, K1Na1 and K1Na0 significantly (P < 0.05) reduced K_{sat} by 43.62%,

215   29.04% and 18.06% compared with CK, respectively (Fig. 2). Additionally, K_{sat} was

216   negatively correlated with CROSS of saline water, increasing the CROSS of the applied

217   saline water generally reduced K_{sat}.
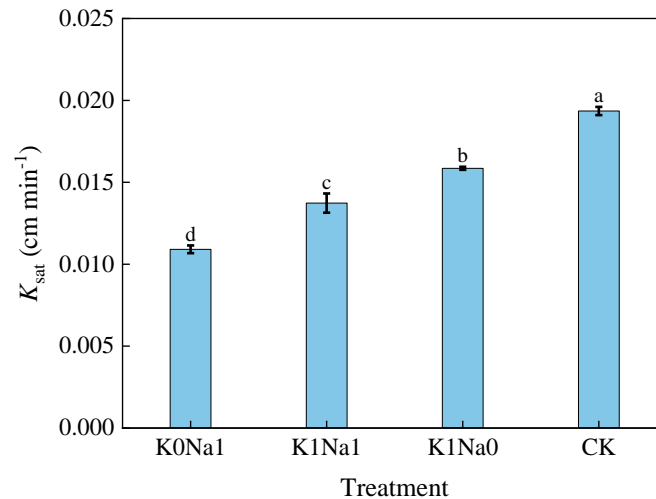
218

219 Fig. 2. Saturated hydraulic conductivity (K_{sat}) under different treatments. K0Na1,

220 K1Na1 and K1Na0 indicate the saline water at EC of 4 dS m^{-1} with K$^+$/Na$^+$ of 0:1, 1:1

221 and 1:0, respectively; CK, deionized water; Different letters after means of K_{sat} indicate

222 statistical differences (P < 0.05) among treatments based on LSD. Bars indicate

223 standard deviations of means.

224 **3.2 Soil water content**

225   Water content increased immediately after each infiltration in all treatments, then

226 gradually decreases and the degree of variation tends to stabilize (Fig. 3). And water

227 content at deeper soil depths was greater than at shallow soil depths at the same time

228 during the whole infiltration period. The water content ranged from 0.39–0.41 and

229 0.40–0.42 cm^3 cm^{-3} at 15 and 30 cm soil depths, respectively. K0Na1 had the highest

230 water content at both 15 and 30 cm soil depths. K1Na1 and K1Na0 were greater than

231 CK at 15 cm soil depth and lower than CK at 30 cm soil depth, and the water content

232 of K1Na1 was higher than K1Na0 at both 15 and 30 cm soil layers.
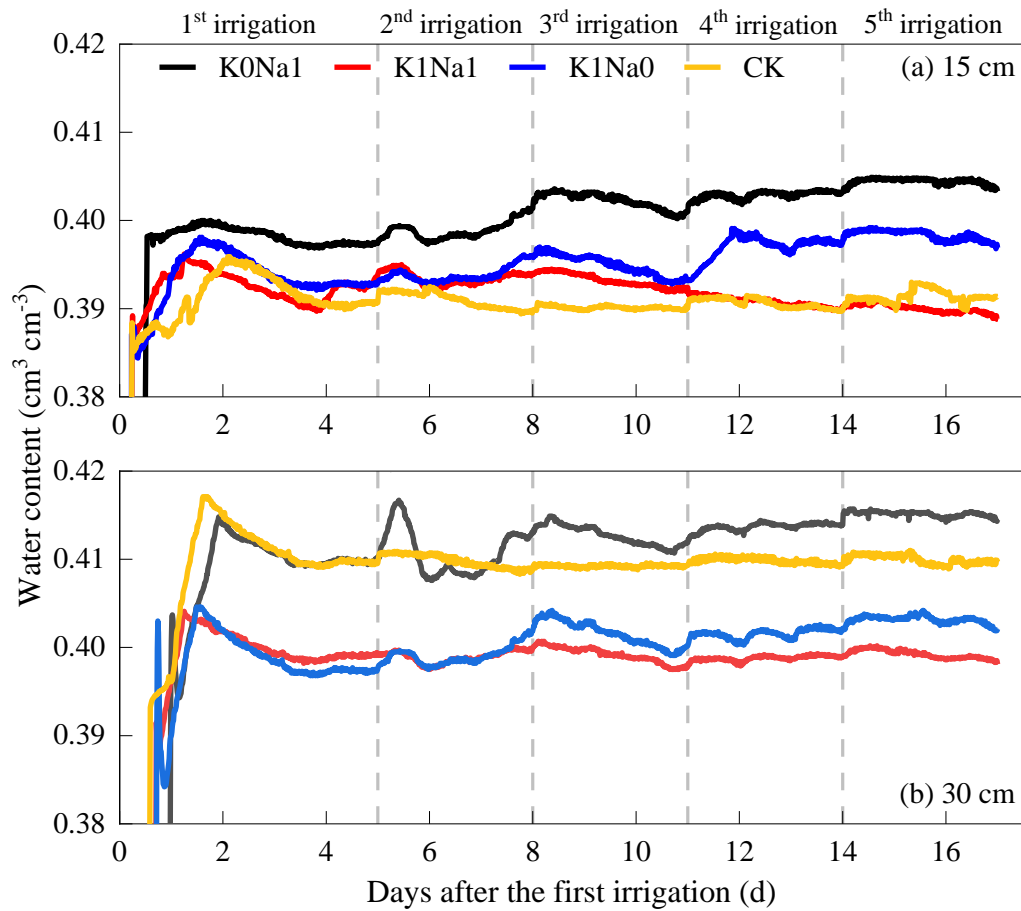
Fig. 3. Variation of water content over time under different treatments at 15 (a) and 30 cm (b) soil depths during the five times of infiltration.

3.3 Soil salination rate (*Rs*) and leaching efficiency (*Le*)

The *Rs* and *Le* under CK were not shown in Fig. 4, because deionized water was used as the control and there was almost no salt contained in the study soil, CK was considered negligible for salt accumulation and leaching. *Rs* peaked at the first infiltration, and approximately 70%–80% of the salt in the saline water was retained in the soil column, after which the subsequent leaching had lower *Rs* values (Fig. 4). The lower the relative concentration of K^+ to Na^+, the larger soil *Rs*. Among the three saline

243 water treatments, K1Na0 had the lowest *Rs* and highest *Le* at five infiltrations.
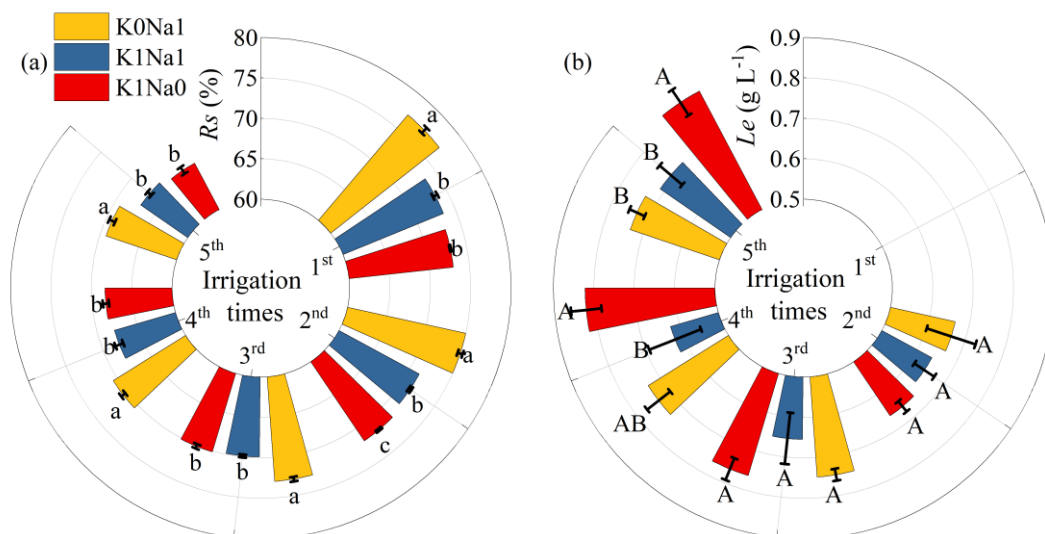
244

245 Fig. 4. Salination rate (*Rs*) (a) and leaching efficiency (*Le*) (b) at five infiltrations under

246 all saline water treatments. K0Na1, K1Na1 and K1Na0 indicate the saline water at EC

247 of 4 dS m^{-1} with K$^+$/Na$^+$ of 0:1, 1:1 and 1:0, respectively; Different lowercase letters

248 followed means of *Rs* indicate statistical differences (P < 0.05) among treatments based

249 on LSD, and different uppercase letters followed means of *Le* indicate statistical

250 differences (P < 0.05) among treatments based on LSD. Bars indicate standard

251 deviations of means.

252 **3.4 Soil bulk electrical conductivity**

253 Bulk electrical conductivity of K0Na1, K1Na1 and K1Na0 ranged from 1.0–2.0

254 dS m^{-1} at 15 cm, 1.5–2.5 dS m^{-1} at 30 cm soil depth (Fig. 5). After the first infiltration,

255 bulk electrical conductivity in 15 cm soil depth peaked, and then exhibited a general

256 downward trend in the following infiltrations. However, more salts were leached to

deeper layers, where salt began to accumulate instead of desalination, and bulk electrical conductivity at 30 cm soil depth gradually increased following the infiltration events. Overall, K0Na1 had the highest bulk electrical conductivity among all treatments at both 15 and 30 cm, and K1Na1 was quite higher than K1Na0.
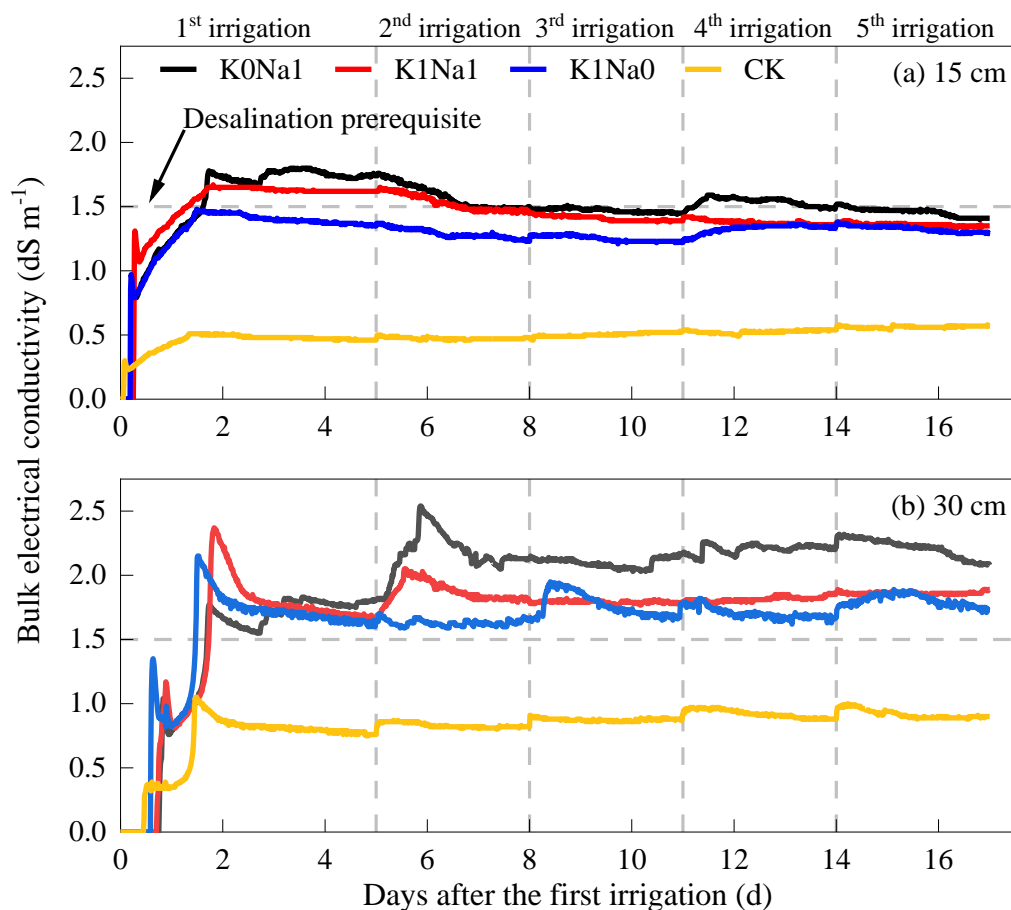
Fig. 5. Variation of bulk electrical conductivity over time under treatments with different K^+/Na^+ at constant EC at 15 (a) and 30 cm (b) soil depths in the period of five times of infiltration. K0Na1, K1Na1 and K1Na0 indicate the saline water at EC of 4 dS m^{-1} with K^+/Na^+ of 0:1, 1:1 and 1:0, respectively; CK, deionized water.

At 15 cm soil depth, K0Na1 reached the soil desalination prerequisite after the fifth infiltration, while K1Na1 reached the desalination prerequisite after the second infiltration, and K1Na0 did not exceed desalination prerequisite during the whole

269   infiltration period. Among all saline water treatments, K1Na0 reduced the desalination

270   time and required leaching volume to reach the standard of desalination. K0Na1,

271   K1Na1 and K1Na0 did not meet the desalination prerequisite at 30 cm soil depth, and

272   the increased volume of infiltration water also increased the bulk electrical conductivity.

273   **3.5 Soil bulk density (*BD*) and total porosity (*TP*)**

274   Soil *BD* varied from 1.30–1.40 g cm^{-3} across all treatments, and *BD* was below

275   1.35 g cm^{-3} at 0–10 and 35–40 cm soil layers, however, over 1.35 g cm^{-3} at 10–35 cm

276   soil depth (Fig. 6). K0Na1 significantly ($P < 0.05$) enhanced soil *BD* throughout the soil

277   column profile compared with CK. *TP* first diminished with soil depth to reach a

278   minimum at about 30–35 cm, and then slightly increased at 35–40 cm. The *TP* of

279   K1Na1 and K1Na0 slightly improved after five times of infiltration, and only K0Na1

280   showed a decline compared with CK. Overall, over the whole infiltration period,

281   K1Na0 was most conducive to the formation of soil pore structure and increasing the

282   total pore volume. The saline water with lower CROSS was beneficial for reducing soil

283   *BD* and increasing *TP*.

284
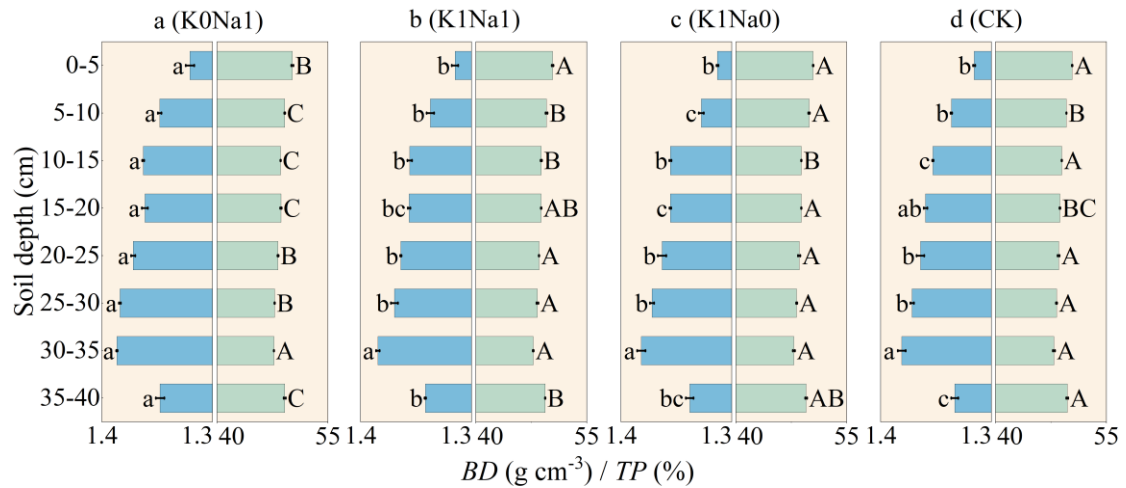
Fig. 6. Soil bulk density (*BD*) and total porosity (*TP*) throughout the soil column profile

under different treatments. K0Na1, K1Na1 and K1Na0 indicate the saline water at EC

of 4 dS m^{-1} with K$^+$/Na$^+$ of 0:1, 1:1 and 1:0, respectively; CK, deionized water; The

blue horizon columns represent *BD*, while the green horizon columns represent *TP*;

Different lowercase letters followed means of *BD* indicate statistical differences (P <

0.05) among treatments based on LSD, and different uppercase letters followed means

of *TP* indicate statistical differences (P < 0.05) among treatments based on LSD. Bars

indicate standard deviations of means.

3.6 Proportion of micropores and proportion of macropores

Micropores were the dominant pores for all treatments, the proportion of

micropores accounting for more than 40% of the total soil volume, however, the

proportion of macropores did not exceed 8% (Fig. 7). The 0–5 cm soil layer had the

lowest proportion of macropores and retained the largest proportion of micropores

compared with other depths. K0Na1 had the highest proportion of micropores and the

299 lowest proportion of macropores. K1Na0 had a greater proportion of macropores in the

300 soil column than CK.

301 Fig. 7. Proportion of micropores and proportion of macropores in total soil volume
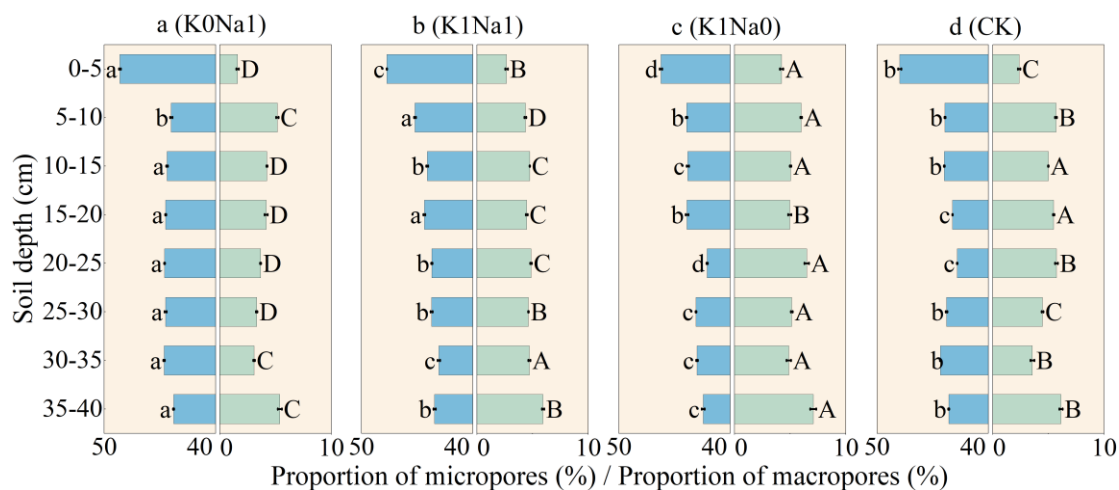
302 Fig. 7. Proportion of micropores and proportion of macropores in total soil volume

303 throughout the soil column profile under different treatments. K0Na1, K1Na1 and

304 K1Na0 indicate the saline water at EC of 4 dS m^{-1} with K$^+$/Na$^+$ of 0:1, 1:1 and 1:0,

305 respectively; CK, deionized water; The blue horizon columns represent proportion of

306 micropores, while the green horizon columns represent proportion of macropores;

307 Different lowercase letters followed means of proportion of micropores indicate

308 statistical differences (P < 0.05) among treatments based on LSD, and different

309 uppercase letters followed means of proportion of macropores indicate statistical

310 differences (P < 0.05) among treatments based on LSD. Bars indicate standard

311 deviations of means.

4 Discussion

4.1 Effects of saline water on soil water movement and redistribution

As a crucial soil hydraulic characteristic, K_{sat} reflects the transportation ability of water and solutes (Braud et al. 2001; Maillard et al. 2011; Albalasmeh et al. 2022). The cation composition and EC of soil solution affect K_{sat} by controlling electrostatic repulsive pressure through surface potential and midpoint potential between adjacent particles, and consequently influence water movement (Fares et al. 2000; Liu et al., 2022b). Specifically, the relative concentration of K^+ to Na^+ in saline water was related to the swelling and dispersion of soil particles (Yu et al. 2016; Zhu et al. 2019). Dispersed clay particles clogged soil macropores to subsequently restrict water transport (Awedat et al., 2021). The Na^+ has a relatively higher ionicity index than K^+, as a result, the low relative concentration of K^+ to Na^+ decreased the degree of covalency in clay-cation bonds, which was detrimental to clay particles aggregation (Marchuk and Rengasamy 2011). Therefore, in our study, the high relative concentration of K^+ to Na^+ promoted the flocculation and stabilization of soil clay particles, resulting in an increased water hydraulic conductivity (Fig. 2).

After a certain period of irrigation, soil moisture redistributed at different depths of soil column (Fig. 3). Soil water moved further down during the phase of water redistribution soon after each irrigation, reducing the water content in the upper soil layers. As the upper soil layers drained, the lower soil layers still had water inflow

332   (Kargas et al., 2021), increasing the water content in the lower soil layers. The results

333   also implicated that the retention of soil water by Na^+ was stronger than that by K^+, the

334   cause may be that Na^+ can increase the thickness of the diffuse-double layers around

335   soil colloids theoretically due to its larger hydrated radius and lower charge than K^+,

336   and the adjacent double layers overlapped to provide more space between layers (He et

337   al., 2015), where, subsequently, more water can be retained (Fig. 3).

338   Additionally, our study showed that K1Na1 was even more beneficial than

339   deionized water for water downward transport (Fig. 3), which was due to that deionized

340   water (CK) (below 0.2 dS m^{-1}) tended to leach soluble minerals and salts, especially

341   Ca^{2+}, from the surface soil layers. This would lead to the reduction of its original solid

342   soil structural stability. In the absence of salt and Ca^{2+}, the dispersed tiny particles filled

343   the smaller pore spaces in soil, reducing even more channels for water flow and

344   exacerbating water retention in deeper soil layers (Ayers and Westcot 1985). However,

345   a lower concentration of soluble salts could increase colloid flocculation, and thereby,

346   improving soil aeration and water conductivity (Tang and She 2016).

347   **4.2 Effects of saline water on soil salination and desalination process**

348   Numerous factors influence soil salt leaching efficiency; for example, increasing

349   EC and reducing SAR definitely improve clay flocculation, which can enhance salt

350   leaching (Ebrahim Yahya et al., 2022). Na^+ is more likely to trigger soil clay dispersion

351   and swelling than K^+, thus Na^+ generally inhibits water infiltration, which is detrimental

352 to salt leaching (Smiles and Smith 2004). Adding K^+ could promote displacement of

353 the adsorbed Na^+, and then decrease Na^+ concentration and salt accumulation in soil

354 solute through leaching.

355   A greater reduction in Na^+ concentration was associated with a higher rate of

356 cation exchange rate, and the slow rate of solute leaching from aggregates reduced the

357 total leaching efficiency (Shaygan et al., 2017). During the leaching process, water flow

358 preferentially passed through the macropores rather than aggregates. The slow water

359 transportation through aggregates induced the slow removal of solutes from the

360 aggregates, leading to a reduced leaching efficiency. In our study, the alternate leaching

361 was implemented to improve solute leaching (Figs. 4 and 5). The soil solutes diffused

362 into the aggregates surface during the rest period, improving salt leaching due to the

363 water flow in macropores (Al-Sibai et al., 1997). Saline water with more K^+ could

364 increase the magnitude of cation exchange due to the substitution of Na^+ on exchange

365 sites by K^+ with lower dispersive potential (Shaygan et al., 2017), the intensive release

366 of cations from the soil further improved salt's leaching efficiency. In addition, the

367 integrity of soil aggregates created by combining clay particles and the other soil

368 components enhanced by K^+ can benefit solute transportation (Marchuk and

369 Rengasamy 2011).

370 **4.3 Effects of saline water on soil pore structure characteristics**

371   The upper soil was longer exposed to water due to the long-term continuous

372   irrigation, causing the particles to swell and the surface layer to loosen (Vaezi et al.

373   2017; Håkansson and Lipiec 2000), and also the decreased BD in the surface layer of

374   soil column (Fig. 6). The subsoil BD increased with depth under the impact of water

375   pressure and self-weight due to the declining pore diameter and pore branching closure

376   (Schjønning et al., 2013). And for soil at the bottom, the loss of soil particles from small

377   holes was responsible for the abrupt reduction in BD (Fig. 6). The value of CROSS in

378   saline water could reflect changes in soil BD and TP, in agreement with the result of

379   Marchuk and Marchuk (2018). The high CROSS implied an increase in the proportion

380   of monovalent exchangeable cations, thickening the double layer at the interface

381   between the clay surface and soil solution. Hence, soil swelling occurred at the expense

382   of water-conducting pores. Additionally, aggregates slaking and subsequent clay

383   dispersion and deposition of clay particles within the pore space contributed to the

384   reduction in TP (Marchuk and Marchuk 2018).

385   Soil macropores play a crucial role in water and solute transport, accounting for

386   85% of the total infiltration volume (Wilson and Luxmoore 1988; Weiler and Naef 2003;

387   Kotlar et al. 2020). For saline water with the same EC, a decrease in K^+ concentration

388   may enhance soil clay dispersion, resulting in the loosening of clay particles from the

389   aggregates. This, in turn, dispersed clay particles moved with water caused the

390   macropores to become blocked, converting them into micropores (Cameira et al., 2003),

391   thus leading to a decrease in the volume of soil macropores (Fig. 7).

5 Conclusion

We explored the effects of the relative ratio of K^+ to Na^+ in saline water on soil hydraulic characteristics and structural stability via a soil column experiment. Irrigation with saline water of K^+/Na^+ of 1:0 caused fewer pore blockages due to soil clay particle dispersion than 0:1, which increased soil saturated hydraulic conductivity. The presence of K^+ accelerated the sustained Na^+ replacement and leaching, alleviating salt accumulation and enhancing leaching efficiency. K^+ positively affected the establishment of soil structure due to the transformation of micropores into macropores, and the ever-increasing unobstructed water-conducting channels sped up water and solute transport. The rational use of saline water with adequate K^+ could help mitigate the structural deterioration caused by Na^+. Appropriate adjustment of the relative concentration of K^+ to Na^+ in saline water during infiltration could ameliorate soil structural properties. In addition to Ca^{2+} and Mg^{2+} (primary concerns in earlier studies), the relative concentration of K^+ to Na^+ is an essential indicator for assessing the suitability of saline water quality for irrigation and should be considered when using saline water.

Data availability

The data will be available upon reasonable request.

Author contributions

Sihui Yan and Tibin Zhang conceived and designed the experiments. Sihui Yan,

Binbin Zhang and Tonggang Zhang led the data processing and statistical analysis, Sihui Yan, Yu Cheng, Chun Wang and Min Luo performed the experiments. Sihui Yan wrote the initial draft. Hao Feng and Kadambot H.M. Siddique contributed to review and editing of the paper.

Competing interests

The contact author has declared that neither they nor their co-authors have any competing interests.

Disclaimer

Publisher's note: Copernicus Publications remains neutral with regard to jurisdictional claims in published maps and institutional affiliations.

Acknowledgments

We are grateful to the reviewers and editors who made constructive comments on this paper.

Financial support

This work was supported by the National Key R&D Program of China (Grant No. 2021YFD1900700), the Innovation Capability Support Program of Shaanxi (Grant no. 2022PT-23), the Key R&D Program of Shaanxi (Grant no. 2023-ZDLNY-53), and China 111 project (B12007).

430 **References**

431 Albalasmeh, A., Mohawesh, O., Gharaibeh, M., Deb, S., Slaughter, L., El Hanandeh, A.: Artificial

432 neural network optimization to predict saturated hydraulic conductivity in arid and semi-arid

433 regions, Catena, 217, 106459, http://dx.doi.org/10.1016/J.CATENA.2022.106459, 2022.

434 Aldaz-Lusarreta, A., Giménez, R., Campo-Bescós, M.A., Arregui, L.M., Virto, I.: Effects of

435 innovative long-term soil and crop management on topsoil properties of a Mediterranean soil

436 based on detailed water retention curves, SOIL, 8, 655-671, http://dx.doi.org/10.5194/SOIL-8-

437 655-2022, 2022.

438 Al-Sibai, M., Adey, M.A., Rose, D.A.: Movement of solute through a porous medium under

439 intermittent leaching, Eur. J. Soil Sci., 48, 711-725, http://dx.doi.org/10.1046/j.1365-

440 2389.1997.00126.x, 1997.

441 Alva, A.K., Sumner, M.E., Miller, W.P.: Relationship between ionic strength and electrical

442 conductivity for soil solutions, Soil Sci., 152, 239-242, https://doi.org/10.1097/00010694-

443 199110000-00001, 1991.

444 Aparicio, J., Tenza-Abril, A.J., Borg, M., Galea, J., Candela, L.: Agricultural irrigation of vine crops

445 from desalinated and brackish groundwater under an economic perspective. A case study in

446 Siġġiewi, Malta, Sci. Total Environ., 650, 734-740,

447 https://doi.org/10.1016/j.scitotenv.2018.09.059, 2019.

448 Awedat, A.M., Zhu, Y., Bennett, J.M., Raine, S.R.: The impact of clay dispersion and migration on

449 soil hydraulic conductivity and pore networks, Geoderma, 404, 115297,

450 http://dx.doi.org/10.1016/J.GEODERMA.2021.115297, 2021.

451   Ayers, R.S., Westcot, D.W.: Water Quality for Agriculture, FAO Irrigation and Drainage Paper 29

452   Rev 1, Rome, Italy.

453   Bao, S.D.: Soil Analysis in Agricultural Chemistry, China Agricultural Press,Beijing, China, 2005

454   (in Chinese).

455   Belkheiri, O., Mulas, M.: The effects of salt stress on growth, water relations and ion accumulation

456   in two halophyte Atriplex species, Environ. Exp. Bot., 86, 17-28,

457   http://dx.doi.org/10.1016/j.envexpbot.2011.07.001, 2013.

458   Bouksila, F., Bahri, A., Berndtsson, R., Persson, M., Rozema, J., Van der Zee, S.E.A.T.M.:

459   Assessment of soil salinization risks under irrigation with brackish water in semiarid Tunisia,

460   Environ. Exp. Bot., 92, 176-185, http://dx.doi.org/10.1016/j.envexpbot.2012.06.002, 2013.

461   Braud, I., Vich, A.I.J., Zuluaga, J., Fornero, L., Pedrani, A.: Vegetation influence on runoff and

462   sediment yield in the Andes region: observation and modelling, J. Hydrol., 254, 124-144,

463   http://dx.doi.org/10.1016/S0022-1694(01)00500-5, 2001.

464   Budhathoki, S., Lamba, J., Srivastava, P., Malhotra, K., Way, T.R., Katuwal, S.: Using X-ray

465   computed tomography to quantify variability in soil macropore characteristics in pastures, Soil

466   Tillage Res., 215, 105194, http://dx.doi.org/10.1016/J.STILL.2021.105194, 2022.

467   Buelow, M.C., Steenwerth, K., Parikh, S.J.: The effect of mineral-ion interactions on soil hydraulic

468   conductivity, Agric. Water. Manag., 152, 277-285,

469   http://dx.doi.org/10.1016/j.agwat.2015.01.015, 2015.

470   Cameira, M.R., Fernando, R.M., Pereira, L.S.: Soil macropore dynamics affected by tillage and

471   irrigation for a silty loam alluvial soil in southern Portugal, Soil Tillage Res., 70, 131-140,

472   http://dx.doi.org/10.1016/S0167-1987(02)00154-X, 2003.

473   Ebrahim Yahya, K., Jia, Z., Luo, W., Yuanchun, H., Ame, M.A.: Enhancing salt leaching efficiency

474   of saline-sodic coastal soil by rice straw and gypsum amendments in Jiangsu coastal area, Ain

475   Shams Eng. J., 13, 101721, http://dx.doi.org/10.1016/J.ASEJ.2022.101721, 2022.

476   Fares, A., Alva, A.K., Nkedi-Kizza, P., Elrashidi, M.A.: Estimation of soil hydraulic properties of a

477   sandy soil using capacitance probes and Guelph Permeameter, Soil Sci. Soc. Am. J., 165, 768-

478   777, https://doi.org/10.1097/00010694-200010000-00002, 2000.

479   Gharaibeh, M.A., Eltaif, N.I., Shunnar, O.F.: Leaching and reclamation of calcareous saline-sodic

480   soil by moderately saline and moderate-SAR water using gypsum and calcium chloride, J. Plant

481   Nutr.   Soil   Sci.,   i.-Z.   Pflanzenernahr.   Bodenkd.,   172,   713–719,

482   http://dx.doi.org/10.1002/jpln.200700327, 2009.

483   Hack-Ten Broeke, M.J.D., Kroes, J.G., Bartholomeus, R.P., Van Dam, J.C., De Wit, A.J.W., Supit,

484   I., Walvoort, D.J.J., Van Bakel, P.J.T., Ruijtenberg, R.: Quantification of the impact of

485   hydrology on agricultural production as a result of too dry, too wet or too saline conditions,

486   SOIL, 2, 391-402, http://dx.doi.org/10.5194/soil-2-391-2016, 2016.

487   Håkansson, I., Lipiec, J.: A review of the usefulness of relative bulk density values in studies of soil

488   structure and compaction, Soil Tillage Res., 53, 71-85, http://dx.doi.org/10.1016/S0167-

489   1987(99)00095-1, 2000.

490   He, Y.B., Desutter, T.M., Casey, F., Clay, D., Franzen, D., Steele, D.: Field capacity water as

491   influenced by Na and EC: Implications for subsurface drainage, Geoderma, 245, 83-88,

492   http://dx.doi.org/10.1016/j.geoderma.2015.01.020, 2015.

493 Hu, X., Li, Z.C., Li, X.Y., Wang, P., Zhao, Y.D., Liu, L.Y., LÜ, Y.L: Soil macropore structure

494 characterized by X-Ray computed tomography under different land uses in the Qinghai Lake

495 watershed, Qinghai-Tibet plateau., Pedosphere, 28, 478-487, http://dx.doi.org/10.1016/S1002-

496 0160(17)60334-5, 2018.

497 Jury, W., Gardner, W.R., Gardner, W.H.: Soil Physics, John Wiley and Sons, New York, USA, 1991.

498 Kargas, G., Soulis, K.X., Kerkides, P.: Implications of hysteresis on the horizontal soil water

499 redistribution after infiltration, Water, 13, 2773-2773, http://dx.doi.org/10.3390/W13192773,

500 2021.

501 Kim, H., Anderson, S.H., Motavalli, P.P., Gantzer, C.J.: Compaction effects on soil macropore

502 geometry and related parameters for an arable field, Geoderma, 160, 244-251,

503 http://dx.doi.org/10.1016/j.geoderma.2010.09.030, 2010.

504 Kotlar, A.M., de Jong van lier, Q., Andersen, H.E., Nørgaard, T., Iversen, B.V.: Quantification of

505 macropore flow in Danish soils using near-saturated hydraulic properties, Geoderma, 375,

506 114479, http://dx.doi.org/10.1016/j.geoderma.2020.114479, 2020.

507 Li, Z.Y., Cao, W.G., Wang, Z.R., Li, J.C., Ren, Y.: Hydrochemical characterization and irrigation

508 suitability analysis of shallow groundwater in Hetao Irrigation District, Inner Mongolia.,

509 Geoscience, 36, 418-426, https://doi.org/10.19657/j.geoscience.1000-8527.2022.012, 2022 (in

510 Chinese).

511 Liu, B.X., Wang, S.Q., Liu, X.J., Sun, H.Y.: Evaluating soil water and salt transport in response to

512 varied rainfall events and hydrological years under brackish water irrigation in the North China

513 Plain, Geoderma, 422, 115954, http://dx.doi.org/10.1016/J.GEODERMA.2022.115954, 2022a.

514   Liu, X.M., Zhu, Y.C., Mclean Bennett, J., Wu, L.S., Li, H.: Effects of sodium adsorption ratio and

515   electrolyte concentration on soil saturated hydraulic conductivity, Geoderma, 414, 115772,

516   http://dx.doi.org/10.1016/J.GEODERMA.2022.115772, 2022b.

517   Luxmoore, R.J.: Micro-, meso-, and macroporosity of soils., Soil Sci. Soc. Am. J., 45, 671-672,

518   http://dx.doi.org/10.2136/sssaj1981.03615995004500030051x, 1981.

519   Maillard, E., Payraudeau, S., Faivre, E., Grégoire, C., Gangloff, S., Imfeld, G.: Removal of pesticide

520   mixtures in a stormwater wetland collecting runoff from a vineyard catchment, Sci. Total

521   Environ., 409, 2317-2324, http://dx.doi.org/10.1016/j.scitotenv.2011.01.057, 2011.

522   Marchuk, A., Marchuk, S.A., Bennett, J.A., Eyres, M.A., Scott, E.: An alternative index to ESP to

523   explain dispersion occurring in Australian soils when Na content is low, National Soils

524   Conference: Proceedings of the 2014 National Soils Conference Soil Science Australia

525   Melbourne, Australia, 2014.

526   Marchuk, A., Rengasamy, P.: Clay behaviour in suspension is related to the ionicity of clay–cation

527   bonds, Appl. Clay Sci., 53, 754-759, http://dx.doi.org/10.1016/j.clay.2011.05.019, 2011.

528   Marchuk, S., Marchuk, A.: Effect of applied potassium concentration on clay dispersion, hydraulic

529   conductivity, pore structure and mineralogy of two contrasting Australian soils., Soil Tillage

530   Res., 182, 35-44, http://dx.doi.org/10.1016/j.still.2018.04.016, 2018.

531   Mckenna, B.A., Kopittke, P.M., Macfarlane, D.C., Dalzell, S.A., Menzies, N.W.: Changes in soil

532   chemistry after the application of gypsum and sulfur and irrigation with coal seam water,

533   Geoderma, 337, 782-791, http://dx.doi.org/10.1016/j.geoderma.2018.10.019, 2019.

534   Prajapati, M., Shah, M., Soni, B.: A review of geothermal integrated desalination: A sustainable

535   solution to overcome potential freshwater shortages, J. Clean. Prod., 326, 129412,

536   http://dx.doi.org/10.1016/J.JCLEPRO.2021.129412, 2021.

537 Qadir, M., Oster, J.D., Schubert, S., Noble, A.D., Sahrawat, K.L.: Phytoremediation of Sodic and

538   Saline - Sodic Soils, Adv. Agron., 96, 197-247, http://dx.doi.org/10.1016/S0065-

539   2113(07)96006-X, 2007.

540 Qadir, M., Sposito, G., Smith, C.J., Oster, J.D.: Reassessing irrigation water quality guidelines for

541   sodicity hazard, Agric. Water. Manag., 255, 107054,

542   http://dx.doi.org/10.1016/J.AGWAT.2021.107054, 2021.

543 Reading, L.P., Lockington, D.A., Bristow, K.L., Baumgartl, T.: Are we getting accurate

544   measurements of Ksat for sodic clay soils? Agric. Water. Manag., 158, 120-125,

545   http://dx.doi.org/10.1016/j.agwat.2015.04.015, 2015.

546 Rengasamy, P., Marchuk, A.: Cation ratio of soil structural stability (CROSS), Soil Res., 49, 280-

547   285, http://dx.doi.org/10.1071/SR10105, 2011.

548 Sahin, U., Eroğlu, S., Sahin, F.: Microbial application with gypsum increases the saturated hydraulic

549   conductivity of saline–sodic soils, Appl. Soil Ecol., 48, 247-250,

550   http://dx.doi.org/10.1016/j.apsoil.2011.04.001, 2011.

551 Schjønning, P., Lamandé, M., Berisso, F.E., Simojoki, A., Alakukku, L., Andreasen, R.R.: Gas

552   diffusion, non-darcy air permeability, and computed tomography images of a clay subsoil

553   affected by compaction, Soil Sci. Soc. Am. J., 77, 1977-1990,

554   http://dx.doi.org/10.2136/sssaj2013.06.0224, 2013.

555 Scudiero, E., Skaggs, T.H., Corwin, D.L.: Simplifying field-scale assessment of spatiotemporal

556   changes of soil salinity, Sci. Total Environ., 587-588, 273-281,

557   http://dx.doi.org/10.1016/j.scitotenv.2017.02.136, 2017.

558   Shaygan, M., Reading, L.P., Baumgartl, T.: Effect of physical amendments on salt leaching

559   characteristics for reclamation, Geoderma, 292, 96-110,

560   http://dx.doi.org/10.1016/j.geoderma.2017.01.007, 2017.

561   Singh, G., Mavi, M.S., Choudhary, O.P., Gupta, N., Singh, Y.: Rice straw biochar application to soil

562   irrigated with saline water in a cotton-wheat system improves crop performance and soil

563   functionality in north-west India, J. Environ. Manage., 295, 113277,

564   http://dx.doi.org/10.1016/J.JENVMAN.2021.113277, 2021.

565   Smiles, D.E., Smith, C.J.: A survey of the cation content of piggery effluents and some consequences

566   of their use to irrigate soils, Soil Res., 42, 231-246, http://dx.doi.org/10.1071/SR03059, 2004.

567   Smith, C.J., Oster, J.D., Sposito,G.: Potassium and magnesium in irrigation water quality assessment,

568   Agric. Water. Manag., 157, 59-64, http://dx.doi.org/10.1016/j.agwat.2014.09.003, 2015.

569   Sposito, G., Oster, J.D., Smith, C.J., Assouline, S.: Assessing soil permeability impacts from

570   irrigation with marginal-quality waters, AB Reviews: Perspectives in Agriculture, Veterinary

571   Science, Nutrition and Natural Resources. 11, 15,

572   http://dx.doi.org/10.1079/PAVSNNR201611015, 2016.

573   Tang, S.Q., She, D.L.: Influence of water quality on soil saturated hydraulic conductivity and

574   infiltration properties, Transactions of the Chinese Society for Agricultural Machinery, 47, 108-

575   114, https://doi.org/10.6041/j.issn.1000-1298.2016.10.015, 2016 (in Chinese).

576   Tsai, W.T., Liu, S.C., Chen, H.R., Chang, Y.M., Tsai, Y.L.: Textural and chemical properties of

577   swine-manure-derived biochar pertinent to its potential use as a soil amendment, Chemosphere,

578   89, 198-203, https://doi.org/10.1016/j.chemosphere.2012.05.085, 2012.

579   Vaezi, A.R., Ahmadi, M., Cerdà, A.: Contribution of raindrop impact to the change of soil physical

580   properties and water erosion under semi-arid rainfalls, Sci. Total Environ., 583, 382-392,

581   http://dx.doi.org/10.1016/j.scitotenv.2017.01.078, 2017.

582   Weiler, M., Naef, F.: Simulating surface and subsurface initiation of macropore flow, J. Hydrol.,

583   273, 139-154, http://dx.doi.org/10.1016/S0022-1694(02)00361-X, 2003.

584   Wilson, G.V., Luxmoore, R.J.: Infiltration, macroporosity, and mesoporosity distributions on two

585   forested watersheds, Soil Sci. Soc. Am. J., 52, 329-335,

586   http://dx.doi.org/10.2136/sssaj1988.03615995005200020005x, 1988.

587   Xu, J., Huang, P.M.: Soil Science, China Agriculture Press, Beijing, China, 2010 (in Chinese).

588   Yang, G., Li, F., Tian, L., He, X., Gao, Y., Wang, Z., Ren, F.: Soil physicochemical properties and

589   cotton (Gossypium hirsutum L.) yield under brackish water mulched drip irrigation, Soil

590   Tillage Res., 199, 104592, https://doi.org/10.1016/j.still.2020.104592, 2020.

591   Yin, C.Y., Zhao, J., Chen, X.B., Li, L.J., Liu, H., Hu, Q.L.: Desalination characteristics and

592   efficiency of high saline soil leached by brackish water and Yellow River water, Agric. Water.

593   Manag., 263, 107461, http://dx.doi.org/10.1016/J.AGWAT.2022.107461, 2022.

594   Yu, Z.H., Liu, X.M., Xu, C.Y., Xiong, H.L., Li, H.: Specific ion effects on soil water movement,

595   Soil Tillage Res., 161, 63-70, http://dx.doi.org/10.1016/j.still.2016.03.004, 2016.

596   Zhang, H.X., Xie, Y.Z.: Alleviating freshwater shortages with combined desert-based large-scale

597   renewable energy and coastal desalination plants supported by Global Energy Interconnection,

598   Glob. Energy Interconnec., 2, 205-213, http://dx.doi.org/10.1016/j.gloei.2019.07.013, 2019.

599   Zhang, T.B., Zhan, X.Y., He, J.Q., Feng, H., Kang, Y.H.: Salt characteristics and soluble cations

600   redistribution in an impermeable calcareous saline-sodic soil reclaimed with an improved drip

601   irrigation, Agric. Water. Manag., 197, 91-99, https://doi.org/10.1016/j.agwat.2017.11.020,

602   2018.

603   Zhu, Y., Bennett, J.M., Marchuk, A.: Reduction of hydraulic conductivity and loss of organic carbon

604   in non-dispersive soils of different clay mineralogy is related to magnesium induced

605   disaggregation, Geoderma, 349, 1-10, https://doi.org/10.1016/j.agwat.2017.11.020, 2019.